Original Article | Neurointervention

https://doi.org/10.3348/kjr.2017.18.2.383
pISSN 1229-6929 · eISSN 2005-8330
Korean J Radiol 2017;18(2):383-391

Korean Journal of Radiology
KJR

Assessment of Arterial Wall Enhancement for Differentiation of Parent Artery Disease from Small Artery Disease: Comparison between Histogram Analysis and Visual Analysis on 3-Dimensional Contrast-Enhanced T1-Weighted Turbo Spin Echo MR Images at 3T

Jinhee Jang, MD[1], Tae-Won Kim, MD[2], Eo-Jin Hwang, MS[1], Hyun Seok Choi, MD[1], Jaseong Koo, MD[2], Yong Sam Shin, MD[3], So-Lyung Jung, MD[1], Kook-Jin Ahn, MD[1], Bum-soo Kim, MD[1]

Departments of [1]Radiology, [2]Neurology, and [3]Neurosurgery, College of Medicine, The Catholic University of Korea, Seoul 06591, Korea

Objective: The purpose of this study was to compare the histogram analysis and visual scores in 3T MRI assessment of middle cerebral arterial wall enhancement in patients with acute stroke, for the differentiation of parent artery disease (PAD) from small artery disease (SAD).

Materials and Methods: Among the 82 consecutive patients in a tertiary hospital for one year, 25 patients with acute infarcts in middle cerebral artery (MCA) territory were included in this study including 15 patients with PAD and 10 patients with SAD. Three-dimensional contrast-enhanced T1-weighted turbo spin echo MR images with black-blood preparation at 3T were analyzed both qualitatively and quantitatively. The degree of MCA stenosis, and visual and histogram assessments on MCA wall enhancement were evaluated. A statistical analysis was performed to compare diagnostic accuracy between qualitative and quantitative metrics.

Results: The degree of stenosis, visual enhancement score, geometric mean (GM), and the 90th percentile (90P) value from the histogram analysis were significantly higher in PAD than in SAD (p = 0.006 for stenosis, < 0.001 for others). The receiver operating characteristic curve area of GM and 90P were 1 (95% confidence interval [CI], 0.86–1.00).

Conclusion: A histogram analysis of a relevant arterial wall enhancement allows differentiation between PAD and SAD in patients with acute stroke within the MCA territory.

Keywords: *Middle cerebral artery; Vessel wall imaging; Enhancement; Histogram analysis; Acute ischemic stroke; Parent artery disease; Small vessel disease; 3T MRI*

INTRODUCTION

Atherosclerosis of intracranial arteries is one of the major causes of acute ischemic stroke (1, 2). Intracranial atherosclerosis could result in two types of ischemic stroke (3-5). The first is a parent artery disease (PAD) or a large vessel disease, which is due to the atherosclerosis in large arteries. The second, a small artery disease (SAD), results from an occlusion of small perforator arteries containing atherosclerotic plaques (6). For middle cerebral artery (MCA), MCA territorial infarcts and striatocapsular infarcts including proximal subcortical infarcts correspond to PAD (7). Conversely, acute distal subcortical infarcts or acute lacunar infarcts on a MCA perforator territory can be categorized as SAD (8). Therefore, detection of offending intracranial arteries could help elucidate pathophysiology of acute ischemic stroke associated with intracranial arterial

Received April 21, 2015; accepted after revision September 1, 2016.

Corresponding author: Hyun Seok Choi, MD, Department of Radiology, Seoul St. Mary's Hospital, College of Medicine, The Catholic University of Korea, 222 Banpo-daero, Seocho-gu, Seoul 06591, Korea.
• Tel: (822) 2258-1439 • Fax: (822) 599-6771
• E-mail: hschoi@catholic.ac.kr

atherosclerosis. Localization of offending arteries could be used for proper treatment guidelines, e.g., choosing between stenting and medical therapy (9-11). Recently, several reports describe visualizing intracranial arterial walls using a high-resolution magnetic resonance imaging (MRI) (12-14). Some studies demonstrated that the enhancement of intracranial arterial walls was a marker for active diseases and a potential marker for culprit atherosclerotic lesions (13, 15). However, their methods of analyses were in general subjective and qualitative. A previously used quantitative measurement of vessel wall enhancement used a region-of-interest (ROI) method (15). Locating ROIs within tiny and thin intracranial arterial wall is not convenient and can be affected by errors and partial volume averaging effects. A recent study suggested that histogram analysis was an objective way to quantify measurements over a ROI method (16). We hypothesized that PAD and SAD in MCA territories had different degrees of enhancement in the M1 segment of MCA due to different locations of offending arteries. We used a histogram analysis, as well as a qualitative analysis as the method of interpretation. The purpose of this study was to compare the histogram analysis results with the visual analysis results in the assessment of MCA wall enhancement in patients with acute stroke.

MATERIALS AND METHODS

Subjects and Diagnostic Categorization

The study design was a retrospective diagnostic accuracy study. Our Institutional Review Board waived the patients' informed consents. From January 2013 to December 2013, 82 consecutive stroke patients were identified by reviewing the stroke registry at a tertiary hospital. They were treated for acute ischemic stroke within 3 days of symptom onset and underwent 3T MRI scans with a 3-dimensional contrast-enhanced T1-weighted turbo spin echo image (3D CE T1-TSE) with a black blood preparation. We excluded patients who met the following criteria: 1) acute ischemic stroke, other than MCA diseases, such as diseases involving carotid bulb, distal internal carotid artery and posterior circulation (n = 19); 2) cardioembolic stroke (n = 13); 3) patients with unknown origins of stroke or other causes such as vasculitis and Moyamoya diseases (n = 11); 4) final diagnosis of transient ischemic attack after stroke workup (n = 9), and 5) the loss of 3D CE T1-TSE raw data or with the poor image quality (n = 5). Therefore, a total of 25 patients of acute infarction in MCA territories were included in this study. Two stroke-specialized neurologists reviewed medical records, relevant clinical findings, and stroke images including diffusion-weighted images (DWI), fluid attenuation inversion recovery (FLAIR) images, and magnetic resonance angiography (MRA). However, they were blinded to the findings in the 3D CE T1-TSE images. PAD and SAD were classified based on lesion patterns (17). In short, PAD included MCA territorial lobar and cortical infarcts, and proximal subcortical infarcts corresponded to PAD (7). SAD included acute distal subcortical infarcts on the ipsilateral MCA perforator territories (8). A single acute lacunar infarction (less than 2 cm in diameter) in an ipsilateral MCA perforator territory was also considered as SAD. Finally, 15 patients were classified as PAD, and the remaining 10 patients were classified as SAD.

Clinical Data

The age, sex, time of the symptom onset, and risk factor information of the patients were collected. The risk factors including hypertension (defined as receiving medication for hypertension or blood pressure > 140/90 mm Hg on repeated measurements), diabetes (defined as receiving medication for diabetes mellitus, fasting blood sugar ≥ 126 mg/dL, or two-hour postprandial blood sugar ≥ 200 mg/dL), previous history of ischemic stroke, smoking history (current smoker or a patient who had quit smoking < 6 months previously), history of alcohol use, and hyperlipidemia (defined as receiving cholesterol-reducing agents or an overnight fasting cholesterol level > 200 mg/dL or low-density lipoprotein ≥ 130 mg/dL), were collected from the stroke registry and medical records. The National Institute of Health Stroke Scale (NIHSS) scores were measured by neurologists at admission.

MR Acquisitions

The MRI and MRA scans were acquired using a 3T MRI machine (Verio; Siemens AG, Erlangen, Germany) with a 16-channel head and neck coil. A routine MRI for stroke patients included DWI, FLAIR, time-of-flight (TOF) MRA for cerebral arteries, contrast-enhanced MRA of supra-aortic arteries, and 3D CE T1-TSE. Intrinsic characteristics of a turbo-spin echo sequence and an applied motion-sensitizing magnetization preparation formed black-blood images of 3D CE T1-TSE (18). 3D CE T1-TSE were acquired 5 minutes after an intravenous injection of 0.1 mmol/kg of gadobutrol (Gadovist; Bayer Healthcare, Germany) at a rate of 1.5 mL/s. The parameters of the 3D CE T1-TSE with

Korean Journal of Radiology
KJR

black blood preparation were a single slab with 192 sagittal slices; voxel size of 0.9 x 0.9 x 0.9 mm without inter-slice gaps; field of view 173 x 250 x 250 mm; repetition time/echo time/flip angle/echo train length = 700 ms/12 ms /120°/42; a number of excitation of 1; and the parallel imaging parameter of 2. The acquisition time of the 3D CE T1-TSE was 6 minutes and 3 seconds.

Qualitative Analysis of 3D CE T1-TSE Images

Two neuroradiologists (with 8-year and 4-year experienced, respectively) reviewed the 3D CE T1-TSE images for visual enhancement scores of the M1 segments in MCA. They were blinded to the patients' clinical and other MR imaging findings. Three orthogonal plane images (axial, coronal, and sagittal images) of the 3D CE T1-TSE images were reviewed to assess the enhancement of MCA walls. A visual analysis of enhancement was based on a three-point scale of the previously suggested grading system (15, 19): grade 0, enhancement similar to or less than that of the intracranial arterial walls without plaque; grade 1, enhancement greater than that of grade 0, but less than that of the pituitary infundibulum; and grade 2, enhancement similar to or greater than that of the pituitary infundibulum. For each patient, the M1 segments of the lesion side and contralateral side of MCA to the relevant stroke were evaluated. Cases with discrepancies between raters were discussed until a consensus was reached.

Quantitative Analysis of TOF-MRA and 3D CE T1-TSE

Subsequently, a 4-year experienced neuroradiologist performed a histogram analysis of 3D CE T1-TSE images two weeks after the qualitative analysis. After reviewing the maximum intensity projection images of TOF-MRA, the rater measured the degree of MCA stenosis. A diameter of the proximal normal M1 segment (M1n) and the most severe stenotic portion of the M1 segment (M1s) were measured. The degree of stenosis was defined using the equation: Degree of stenosis (%) = (M1n - M1s) / M1n (20).

To compare the stenosis and enhancement degree for markers of offending arteries, five consecutive sagittal source images (3D CE T1-TSE) containing the most severe MCA stenosis were used for drawing ROIs after reviewing the TOF-MRA images (Fig. 1A). The ROIs were drawn on the outer margin of MCA, which included the MCA wall and lumen (Fig. 1A). Therefore, the volume of interest (VOI) was a summation of five consecutive ROIs including the arterial walls and lumens, and the voxel data was displayed on a histogram (Fig. 1B). The signal intensities of all voxels in VOIs were normalized by a mean signal intensity of the genu of corpus callosum, which was located out of the MCA territory (21). We analyzed two different metrics representing VOIs i.e., geometric means (GM) and percentile

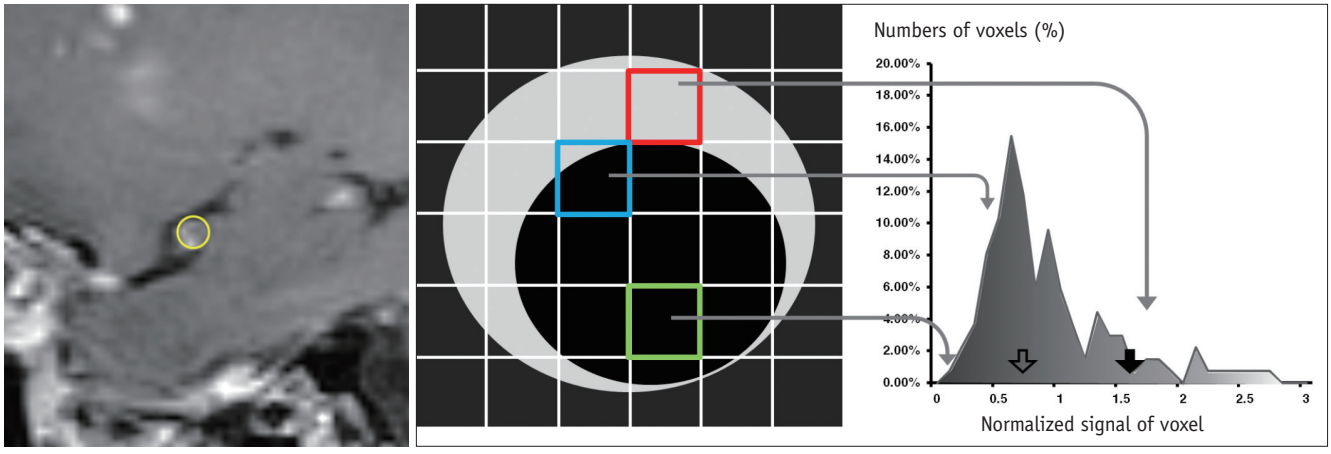

A B

Fig. 1. Example of histogram analysis of MCA wall enhancement.
Case with eccentric enhancement in source image **(A)** of 3D CE T1-TSE and corresponding region-of-interest (yellow circle in **A**) for enhancing middle cerebral artery including wall and its lumen. Left side of scheme **(B)** is scheme of sagittal M1 segment and matching voxel of 3D CE T1-TSE. Enhancing wall with variable degrees of thickness is presented in gray, and lumen of MCA and surrounding tissues are presented in black. Voxel intensity was decided from mean values of internal tissues, and depended on ratio of vessel wall, lumen and surrounding tissues. Voxel has mixed contents of enhancing wall and lumen with variable degrees (blue box). As result, voxels had variable degrees of signals from those of enhancing walls only (red box) to those of lumen only (green box). Example of histogram of normalized signal of VOI is located on right side of scheme. Shaded area under histogram represents relative signal intensities. Two histogram parameters, 90th percentile (solid arrow) and geometric mean (empty arrow) are marked. MCA = middle cerebral artery, VOI = volume of interest, 3D CE T1-TSE = 3-dimensional contrast-enhanced T1-weighted turbo spin echo image

values (Fig. 1B). Because the distributions of histograms were right-side skewed, GM was a better representative value than the arithmetic mean (22). The GM of a VOI, which was a center of histogram mass, was calculated using a log-transformation. We compared 20 different percentile values of VOIs from the 5th to 100th percentiles with increments of five percentiles. Then, the 90th percentile (90P) was chosen as an optimal discriminator and used for analyses. The measurements of a quantitative analysis were performed by ImageJ (ver 1.47, U. S. National Institutes of Health, Bethesda, MD, USA; http://imagej.nih.gov/ij/) and by a commercially available software (Excel 2007, Microsoft).

Statistical Analysis

The differences of demographics, risk factors, and NIHSS scores between the two groups were analyzed by a chi-square and Mann-Whitney U test. Measurements of the degree of stenosis, visual enhancement score, GM and 90P values of the VOIs between two groups were compared using a Mann-Whitney U test. A diagnostic performance was analyzed by a receiver operating characteristic (ROC) curve: the volume of VOI, the degree of stenosis, the enhancement score, GM and the 90P value of VOI. The cut-off values with the greatest Youden's J index were chosen for determining sensitivity and specificity. Comparisons of the areas under the ROC curves (AUCs) were performed by Delong's test, with corrections for multiple comparisons by a Bonferroni correction.

A commercially available software (MedCalc for Windows, Version 13.0.0.0; MedCalc Software, Mariakerke, Belgium) was used for analysis. The statistical significance was set to be two-tailed p value < 0.05.

RESULTS

Qualitative Analysis

Baseline characteristics of the 15 PAD patients and 10 SAD patients were presented in Table 1. Demographics and risk factors showed no significant group-wise differences. The NIHSS score was significantly higher in PAD than in SAD (Table 1). The visual enhancement scores of the PAD group were statistically higher than those of the SAD group. In the PAD group, The visual enhancement scores of the lesion side were significantly higher than those of the contralateral side in the PAD group, as compared to patients with SAD (Table 2). The PAD group also showed a higher stenosis degree of M1 segment in the lesion side than in the contralateral side. On the other hand, the mean stenosis degree of the lesion and contralateral sides in SAD were minimal (< 11 %).

Quantitative and Histogram Analysis

The degree of the lesion side MCA stenosis was significantly higher in PAD than in SAD. In the PAD group, the MCA stenosis in the ipsilateral side was significantly higher than that in the contralateral side (Table 2). The enhancement of the ipsilateral MCA measured by GM and 90P were higher in PAD than in SAD. Moreover, the GM and 90P of the ipsilateral MCA were higher than those of the contralateral side in the PAD patients (Fig. 2); whereas, the GM and 90P were not different between lesion and contralateral sides in the SAD patients (Table 2, Fig. 2). The different shapes in the histograms were found between PAD

Table 1. Demographics and Risk Factors of Two Groups

	PAD (n = 15)	SAD (n = 10)	*P*
Age, years	62, 52–71	61, 57–80	0.934
Sex, M/F	5/10	5/5	0.405
Side, right/left	6/9	3/7	0.9322
NIHSS	4, 3–6	1, 0–1	0.005*
Interval between symptom onset and MR imaging, hours	26.21, 20.15–55.27	25.28, 13.74–77.88	0.782
Hypertension, n	8 (53)	4 (40)	0.688
Diabetes, n	11 (73)	8 (80)	1.000
Hyperlipidemia, n	13 (87)	7 (70)	0.358
Current smoker, n	4 (27)	3 (30)	0.551
Previous ischemic stroke, n	4 (27)	0 (0)	0.125

Figures in parentheses are percentages. Age, NIHSS, interval between onset time to imaging were presented by median and inter-quartile ranges. Others were presented patient numbers in each category. *p < 0.05 by Wilcoxon's signed rank test. NIHSS = National Institute of Health Stroke Scale, PAD = parent artery disease, SAD = small artery disease

Korean Journal of Radiology
KJR

Table 2. Qualitative and Quantitative Analysis of M1 Segment of MCA

Method of Measurements			PAD	SAD	*P*
Visual enhancement score,† n (%)	Lesion side	0	1 (6.7)	5 (50)	< 0.001*
		1	0 (0)	4 (40)	
		2	14 (93.3)	1 (10)	
	Contralateral side	0	10 (66.7)	4 (40)	1.000
		1	5 (33.3)	6 (60)	
		2	0 (0)	0 (0)	
Volume of measured M1 (mm^3)	Lesion side		69.26, 59.05–81.65	66.70, 43.74–86.02	0.454
	Contralateral side		67.07, 62.69–78.73	64.88, 56.86–72.90	0.304
Stenosis† (%)	Lesion side		53.7, 11–66.67	8.17, 1.87–12.99	0.006*
	Contralateral side		10.61, 4.04–12.85	8.14, 2.54–14.75	0.803
GM†	Lesion side		0.68, 0.56–0.82	0.47, 0.29–0.70	< 0.001*
	Contralateral side		0.37, 0.31–0.52	0.32, 0.26–0.37	0.183
90P†	Lesion side		1.15, 0.96–1.38	0.62, 0.57–0.71	< 0.001*
	Contralateral side		0.62, 0.57–0.67	0.58, 0.50–0.68	0.605

Volume of measured M1, stenosis, GM and 90P were presented in median and interquartile ranges. Visual enhancement score: grade 0, enhancement was similar to or less than that of intracranial arterial walls without plaque in same individual; grade 1, enhancement was greater than that of grade 0 but less than that of pituitary infundibulum; and grade 2, enhancement was similar to or greater than that of infundibulum. *Parameters were significantly different between lesion side and contralateral side in Mann-Whitney U test ($p < 0.001$), †Visual enhancement score, Stenosis, GM, and 90P were significantly different between lesion side and contralateral side in large vessel disease group in Wilcoxon signed rank test ($p < 0.001$). GM = geometric mean, MCA = middle cerebral artery, PAD = parent artery disease, SAD = small artery disease, VOI = volume of interest, 90P = 90th percentile of normalized signal of VOI of M1

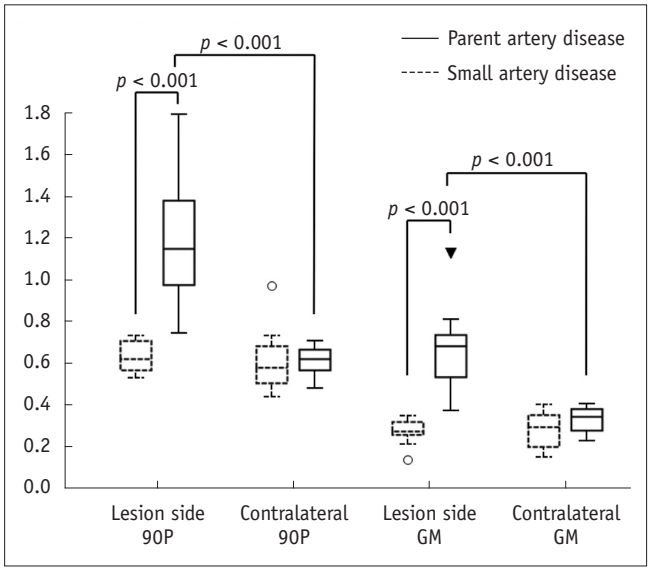

Fig. 2. Box and whisker plot of 90P and GM for lesion and contralateral side of M1 in both groups. Lesion side 90P was significantly higher in PAD group than in SAD group. Contralateral side 90P showed no significant difference between two groups. Lesion side 90P and GM of PAD group was significantly higher than that of SAD group. In PAD group, lesion side GM and 90P was significantly higher than contralateral side GM. GM = geometric means, PAD = parent artery disease, SAD = small artery disease, 90P = 90th percentile

and SAD groups (Figs. 3, 4). The histogram from the PAD patients was more right-side skewed than that from the SAD patients.

ROC Curve Analysis

The ROC curve analysis (Table 3) results suggested that both GM and 90P of MCA enhancement were excellent discriminators in differentiating PAD from SAD, with both sensitivity and specificity of 100%. The AUC values for GM and 90P in our study sample were greater than that of stenosis of the lesion side M1 but showed no statistical significance after multiple-comparison corrections ($p = 0.274$). The AUCs of GM and 90P were also not significantly different from that of visual enhancement score ($p = 0.914$).

DISCUSSION

In this study, both quantitative and qualitative assessments of M1 segment of MCA showed stenosis and wall enhancement in PAD, which was presumed to be an offending artery of the PAD patients; these changes were not evident for SAD patients and the differences were significant. Our study showed a substantial diagnostic performance of these parameters to differentiate PAD from SAD. Especially, the quantitative metrics such as GM and 90P showed excellent sensitivity (100%) and specificity (100%) in diagnosis of PAD over SAD. This finding was concordant with previous studies, which have suggested that the contrast enhancement could be a marker for active diseases in intracranial arteries (12, 15). However, no

previous studies have compared the enhancement between groups with different causes of stroke.

Imaging of intracranial atherosclerosis is still challenging because of the small dimensions of intracranial arterial walls and limited contrast-to-noise ratio (23). Currently, enhancement of vessel walls is a widely-accepted marker of culprit lesions, which is considered an active atherosclerotic lesion (13, 15). For assessing the intracranial arterial wall enhancement, black-blood images and high spatial resolution should be achieved. Although we used a sub-millimeter-sized voxel, even pathologic MCA wall thickness could be far smaller than the voxel size. In this case, the partial volume averaging effects among the vascular walls, lumen and the surrounding tissues are inevitable. In addition, locating ROIs within the vessel wall was challenging. To overcome this problem, we drew VOIs to include both the MCA lumen and walls instead of drawing small ROIs within the arterial walls (Fig. 1). Subsequently, we analyzed the whole voxels within the identified VOIs using a histogram analysis. Qiao et al. (15) quantified the degree of intracranial arterial wall enhancement using ROIs within the vessel walls. They quantified the degree of enhancement by obtaining both non-enhanced and contrast-enhanced images. Their method was straightforward for quantifying the degree of the intracranial artery enhancement. However, potential problems include longer acquisition times, delicacy of selecting ROIs for subtle enhancement of the vessel walls, and the mis-registration problem due to the repeated manual-drawing of ROIs on the two different images. Therefore, we used a histogram

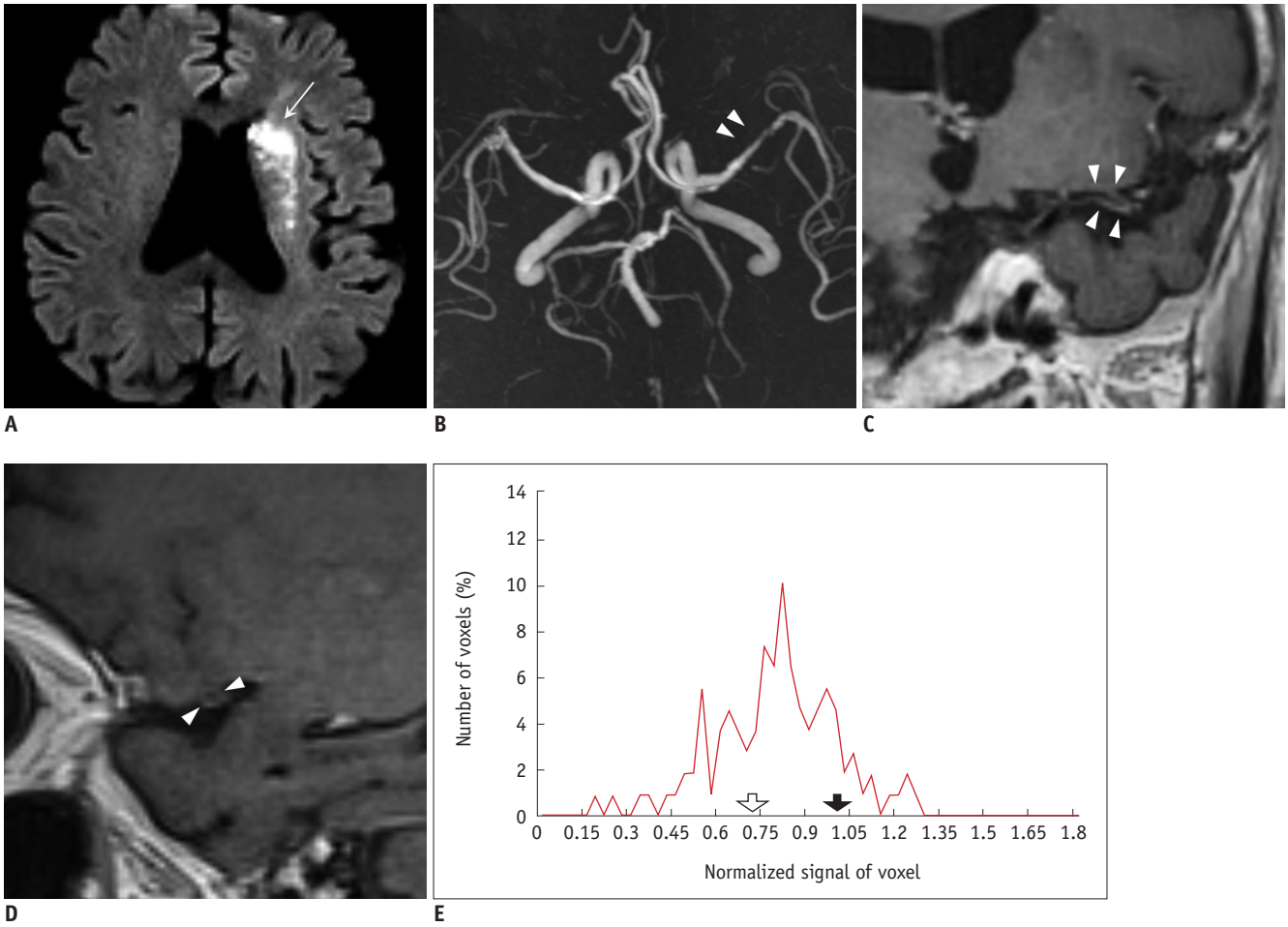

Fig. 3. Case of PAD. 82-year-old woman visited emergency room for tendency to fall to right side. DWI showed patchy area of hyperintensity (arrow on **A**) of left frontal white matter and centrum semiovale. Mild stenosis (44%) was noted in distal M1 segment of left MCA (arrowheads on **B**). Note long segmental enhancement (arrowheads on **C** and **D**) along stenotic segment of left MCA on multiplanar reformatted image **(C)** and sagittal image **(D)** of 3D CE T1-TSE. On histogram analysis of lesion side **(E)**, 90P (solid arrow on **E**) was 1.015, which was higher than our cut-off value of 0.73. Lesion side GM (empty arrow on **E**) was 0.738. Cut-off of GM was 0.346. DWI = diffusion-weighted images, GM = geometric means, MCA = middle cerebral artery, PAD = parent artery disease, 3D CE T1-TSE = 3-dimensional contrast-enhanced T1-weighted turbo spin echo image, 90P = 90th percentile

Korean Journal of Radiology
KJR

analysis method to avoid these problems.

Our results showed that the MCA enhancement was an accurate discriminator of PAD from SAD as the stenosis of M1 segment. A study based on autopsy suggested that intracranial atherosclerosis and the resultant stenosis could be associated with acute ischemic stroke (24). The following

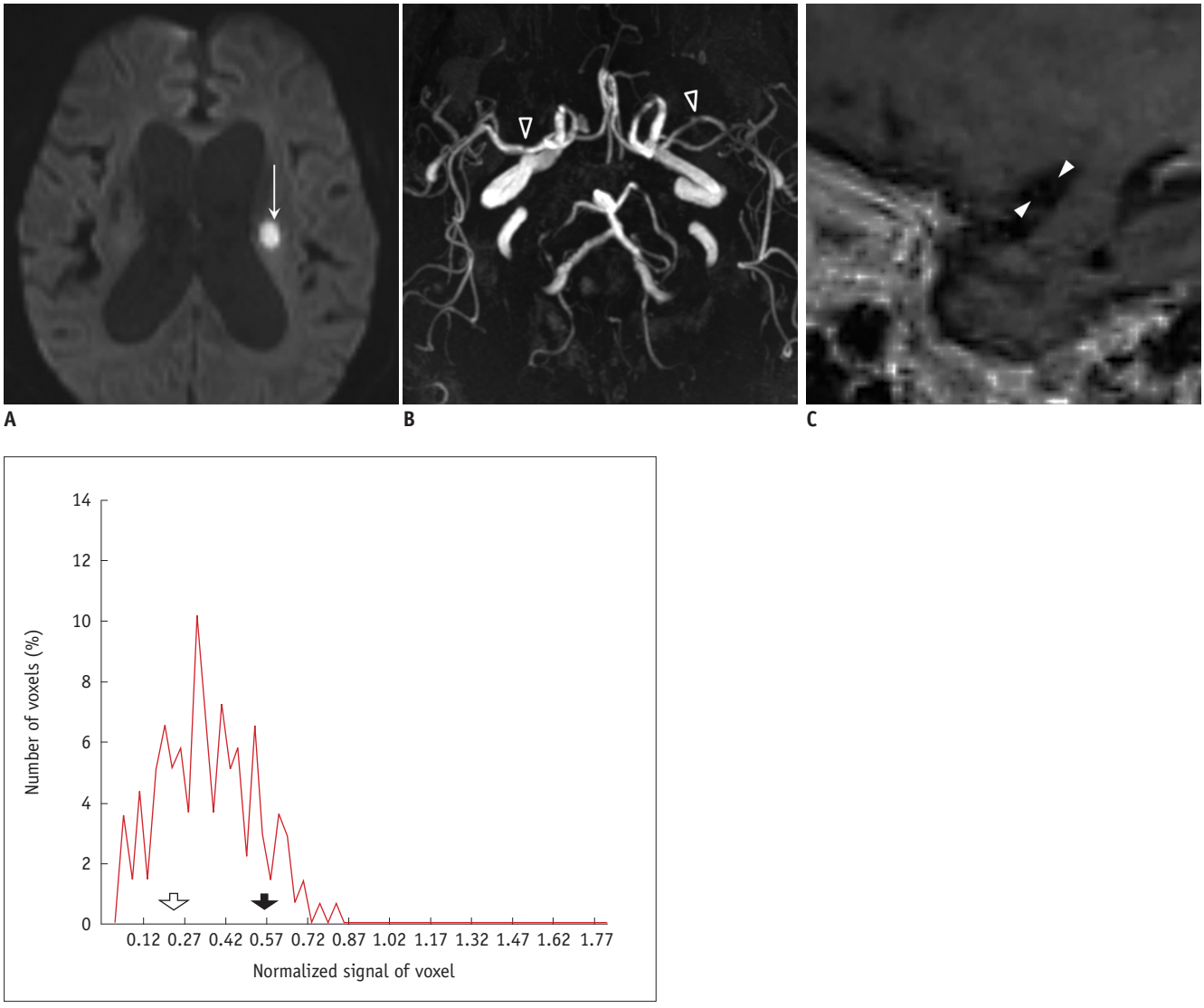

Fig. 4. Case of SAD. 86-year-old woman visited emergency room for dysarthria. DWI showed small acute ischemic stroke lesion in left periventricular white matter (arrow on **A**). Minimal irregular contour (arrowheads) of M1 segment of left MCA was visible **(B)**, and degree of stenosis was 20%. On sagittal image **(C)**, enhancement score was 0. Histogram analysis of lesion side M1 **(D)** showed low 90P (solid arrow, 0.568) and low GM (empty arrow, 0.256) in lesion side M1. DWI = diffusion-weighted image, GM = geometric means, MCA = middle cerebral artery, SAD = small artery disease, 90P = 90th percentile

Table 3. Receiver Operating Characteristic Analysis of Vessel Wall Enhancement and Stenosis for Discrimination of PAD versus SAD

Method of Measurements	AUC	Criterion	Sensitivity (%)	Specificity (%)
Geometric mean	1 (0.86–1)	> 0.35	100 (78.2–100)	100 (69.2–100)
Lesion side 90P	1 (0.86–1)	> 0.73	100 (78.2–100)	100 (69.2–100)
Visual enhancement score	0.90 (0.72–0.98)	> 1	93.33 (68.1–99.8)	90.0 (55.5–99.7)
Stenosis of lesion side M1	0.83 (0.63–0.95)	> 20.25%	66.7 (38.4–88.2)	100 (69.2–100)
Volume of measured M1	0.59 (0.38–0.78)	> 44 mm^3	100 (78.2–100)	30 (6.7–65.2)

Numbers within parentheses are 95% CI. AUC = area under the receiver operating characteristic curve, CI = confidence interval, PAD = parent artery disease, SAD = small artery disease, 90P = 90th percentile

studies with MR images suggested that the atherosclerotic lesions of the intracranial arteries showed not only stenosis of the affected arteries but also the wall enhancement (5, 13, 25). Stenosis and enhancement were major findings of the intracranial arterial atherosclerotic lesions. Our results from comparing the lesion and the contralateral sides revealed a significantly different enhancement in PAD. This result also suggests the clinical significance of intracranial artery enhancement, which may serve as a marker for an active inflammation of culprit arteries. A previous study showed that the enhancement score or the degree of enhancement were more suggestive of a culprit atherosclerotic lesion than the intracranial artery stenosis (15). Another recent study reported the value of plaque eccentricity for symptomatic atherosclerotic lesions of intracranial arteries over the plaque enhancement (26). In this study, the diagnostic performance of GM and 90P was not significantly different from that of stenosis. Future study is needed to resolve these controversial observations.

Atherosclerotic changes in intracranial arteries could induce acute lacunar infarctions if they involved perforator artery ostia (5). Yoon et al. (8) suggested that small subcortical infarcts in MCA territory comprised two different entities according to its relative distance from MCA. Their study suggested that the characteristics of the atherosclerotic plaques in M1 of MCA were different between the two entities. It is possible that PAD and SAD were in a spectrum of the MCA diseases, which had a range of severity and extent of the active inflammatory atherosclerotic changes in M1 of MCA and in its branches. Future studies would be needed to prove the variable features of the MCA atherosclerosis.

This study had several limitations. First, due to the retrospective nature of the study, an uncontrolled bias could have been introduced. However, we systematically reviewed the clinical and imaging findings to include and exclude patients who strictly met our criteria. Therefore, more homogeneous populations representing PAD and SAD could be enrolled in this study. Second, the number of the included patients was relatively small, although previous studies also had similar patient numbers. Third, a pathologic correlation of the M1 segment enhancement was not established. Fourth, the MR sequences used for our study were not specifically designed for vessel wall imaging. Therefore, the set echo time was not adequate (relatively short, 12 ms), which may have introduced slow flow artifacts resulting in pseudo-enhancement (27). Also, the vessel walls were not very clear or well delineated from the surroundings. Additionally, our routine MR protocol did not include any non-enhanced 3D T1-weighted TSE images. It was thus difficult to identify the source of true vessel wall enhancement before contrast administration, whether an effect of slow flow or hyper-intense plaques. Further studies on the comparison of histogram analyses between the pre- and post-contrast images are required. Lastly, we did not measure the degree of enhancement of offending artery of SAD. The luminal diameter and wall thickness of lenticulostriate arteries were beyond the resolution of current MR images. Instead, we observed loss of enhancement at the M1 segment of SAD patients, which could be another source of an offending artery.

In conclusion, our qualitative and quantitative analyses revealed higher M1 segment enhancement in PAD than in SAD. Our study also showed that the intracranial wall enhancement was another important discriminator of PAD from SAD, as well as the presence of stenosis. The histogram analysis is an objective method for quantifying the intracranial artery enhancement.

REFERENCES

1. Feldmann E, Daneault N, Kwan E, Ho KJ, Pessin MS, Langenberg P, et al. Chinese-white differences in the distribution of occlusive cerebrovascular disease. *Neurology* 1990;40:1541-1545
2. Wityk RJ, Lehman D, Klag M, Coresh J, Ahn H, Litt B. Race and sex differences in the distribution of cerebral atherosclerosis. *Stroke* 1996;27:1974-1980
3. Adams HP Jr, Bendixen BH, Kappelle LJ, Biller J, Love BB, Gordon DL, et al. Classification of subtype of acute ischemic stroke. Definitions for use in a multicenter clinical trial. TOAST. Trial of Org 10172 in Acute Stroke Treatment. *Stroke* 1993;24:35-41
4. Skarpathiotakis M, Mandell DM, Swartz RH, Tomlinson G, Mikulis DJ. Intracranial atherosclerotic plaque enhancement in patients with ischemic stroke. *AJNR Am J Neuroradiol* 2013;34:299-304
5. Bodle JD, Feldmann E, Swartz RH, Rumboldt Z, Brown T, Turan TN. High-resolution magnetic resonance imaging: an emerging tool for evaluating intracranial arterial disease. *Stroke* 2013;44:287-292
6. Wardlaw JM. What is a lacune? *Stroke* 2008;39:2921-2922
7. Kim JS, Yoon Y. Single subcortical infarction associated with parental arterial disease: important yet neglected sub-type of atherothrombotic stroke. *Int J Stroke* 2013;8:197-203
8. Yoon Y, Lee DH, Kang DW, Kwon SU, Kim JS. Single subcortical infarction and atherosclerotic plaques in the middle cerebral artery: high-resolution magnetic resonance

imaging findings. *Stroke* 2013;44:2462-2467
9. Chimowitz M, Lynn MJ, Derdeyn CP, Turan TN, Fiorella D, Lane BF, et al. Stenting versus aggressive medical therapy for intracranial arterial stenosis. *N Engl J Med* 2011;365:993-1003
10. Turan TN, Cotsonis G, Lynn MJ, Wooley RH, Swanson S, Williams JE, et al. Intracranial stenosis: impact of randomized trials on treatment preferences of US neurologists and neurointerventionists. *Cerebrovasc Dis* 2014;37:203-211
11. Ding D, Starke RM, Crowley RW, Liu KC. Role of stenting for intracranial atherosclerosis in the post-SAMMPRIS era. *Biomed Res Int* 2013;2013:304320
12. Klein IF, Lavallée PC, Touboul PJ, Schouman-Claeys E, Amarenco P. In vivo middle cerebral artery plaque imaging by high-resolution MRI. *Neurology* 2006;67:327-329
13. Swartz RH, Bhuta SS, Farb RI, Agid R, Willinsky RA, Terbrugge KG, et al. Intracranial arterial wall imaging using high-resolution 3-Tesla contrast-enhanced MRI. *Neurology* 2009;72:627-634
14. Klein IF, Lavallée PC, Mazighi M, Schouman-Claeys E, Labreuche J, Amarenco P. Basilar artery atherosclerotic plaques in paramedian and lacunar pontine infarctions: a high-resolution MRI study. *Stroke* 2010;41:1405-1409
15. Qiao Y, Zeiler SR, Mirbagheri S, Leigh R, Urrutia V, Wityk R, et al. Intracranial plaque enhancement in patients with cerebrovascular events on high-spatial-resolution MR images. *Radiology* 2014;271:534-542
16. Heye T, Merkle EM, Reiner CS, Davenport MS, Horvath JJ, Feuerlein S, et al. Reproducibility of dynamic contrast-enhanced MR imaging. Part II. Comparison of intra- and interobserver variability with manual region of interest placement versus semiautomatic lesion segmentation and histogram analysis. *Radiology* 2013;266:812-821
17. Lee DK, Kim JS, Kwon SU, Yoo SH, Kang DW. Lesion patterns and stroke mechanism in atherosclerotic middle cerebral artery disease: early diffusion-weighted imaging study. *Stroke* 2005;36:2583-2588
18. Nguyen TD, De Rochefort L, Spincemaille P, Cham MD, Weinsaft JW, Prince MR, et al. Effective motion-sensitizing magnetization preparation for black blood magnetic resonance imaging of the heart. *J Magn Reson Imaging* 2008;28:1092-1100
19. van der Kolk AG, Zwanenburg JJ, Brundel M, Biessels GJ, Visser F, Luijten PR, et al. Intracranial vessel wall imaging at 7.0-T MRI. *Stroke* 2011;42:2478-2484
20. Samuels OB, Joseph GJ, Lynn MJ, Smith HA, Chimowitz MI. A standardized method for measuring intracranial arterial stenosis. *AJNR Am J Neuroradiol* 2000;21:643-646
21. Natori T, Sasaki M, Miyoshi M, Ohba H, Katsura N, Yamaguchi M, et al. Evaluating middle cerebral artery atherosclerotic lesions in acute ischemic stroke using magnetic resonance T1-weighted 3-dimensional vessel wall imaging. *J Stroke Cerebrovasc Dis* 2014;23:706-711
22. Bland JM, Altman DG. Transformations, means, and confidence intervals. *BMJ* 1996;312:1079
23. Dieleman N, van der Kolk AG, Zwanenburg JJ, Harteveld AA, Biessels GJ, Luijten PR, et al. Imaging intracranial vessel wall pathology with magnetic resonance imaging: current prospects and future directions. *Circulation* 2014;130:192-201
24. Mazighi M, Labreuche J, Gongora-Rivera F, Duyckaerts C, Hauw JJ, Amarenco P. Autopsy prevalence of intracranial atherosclerosis in patients with fatal stroke. *Stroke* 2008;39:1142-1147
25. Ryu CW, Jahng GH, Kim EJ, Choi WS, Yang DM. High resolution wall and lumen MRI of the middle cerebral arteries at 3 Tesla. *Cerebrovasc Dis* 2009;27:433-442
26. Dieleman N, Yang W, Abrigo JM, Chu WC, van der Kolk AG, Siero JC, et al. Magnetic resonance imaging of plaque morphology, burden, and distribution in patients with symptomatic middle cerebral artery stenosis. *Stroke* 2016;47:1797-1802
27. Qiao Y, Steinman DA, Qin Q, Etesami M, Schär M, Astor BC, et al. Intracranial arterial wall imaging using three-dimensional high isotropic resolution black blood MRI at 3.0 Tesla. *J Magn Reson Imaging* 2011;34:22-30